ORIGINAL ARTICLE

Inhibition of copper corrosion by bipyrazole compound in aerated 3% NaCl

B. Hammouti [a],[*], A. Dafali [a], R. Touzani [a,b], M. Bouachrine [c]

[a] *Laboratoire de Chimie Appliquée & Environnement, LCAE-URAC18, Faculté des Sciences, Université Mohammed Premier, BP48087, 60 046 Oujda, Morocco*
[b] *Université Mohammed Premier, Faculté Pluridisciplinaire Nador, Morocco*
[c] *UMIM, Faculté Polydisciplinaire de Taza, Université Sidi Mohamed Ben Abdellah, Taza, Morocco*

Abstract The corrosion behaviour of copper in aerated 3% NaCl solution was investigated by rotating electrode at various rates. The reduction of O_2 obeys the Levich equation. The inhibition of the copper corrosion in aerated 3% NaCl solution was studied by using potentiodynamic polarisation and linear polarisation resistance (LRP) in the presence of different concentrations of a bipyrazolic compound named *N,N*-bis (3-carbomethoxy-5-methylpyrazol-1-ylmethyl) cyclo-hexylamine (BiPyA). The presence of this compound in the solution decreases the corrosion current density and increases the linear resistance polarisation. The inhibition efficiencies obtained from cathodic Tafel plots and LRP methods are in good agreement. BiPyA compound presents an efficient inhibitor of copper corrosion, acts as a mixed-type inhibitor and adsorbs on the copper surface according to the Langmuir isotherm model.

1. Introduction

Copper and its alloys are the dominant materials for sea water systems in many countries. The annual world production of copper water tubing is ∼500,000 tonnes, equivalent to ∼1.25 billion m or 0.75 million miles. The reasons for this enormous consumption of copper plumbing tube are its excellent corrosion resistance, its ease of fabrication during installation, and hence low-installation costs, and additionally, its contribution to health and the maintenance of healthy water. Further, copper is seen as environmentally friendly due to its potential to be 100% recycled (Revie, 2000; Scharnweber, 2008). Because of the aggression of solutions, particularly when they contain chloride ions, inhibitors are commonly used to reduce the corrosive attack on metallic materials. The review including
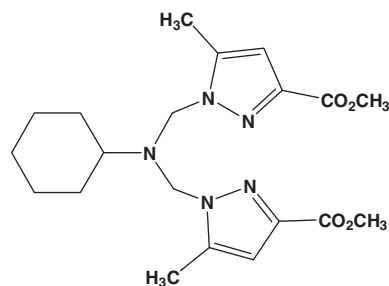
Figure 1   Molecular structure of BiPyA.

extensive listing of various types of organic inhibitors has been published (Tuck et al., 2010).

Different corrosion inhibitors were used to control and reduce corrosion of metals in corrosive media. Due to the toxicity of most inorganic corrosion inhibitors, such as chromates and nitrites and also because of restrictive environmental regulations, these inhibitors are being replaced by new environment-friendly organic compounds.

Among the widely used inhibitors, pyrazolic compounds and their derivatives for inhibiting copper corrosion in aqueous chloride solution, have successfully to drawn the attention of many researchers (Aouniti et al., 1996; Badawy et al., 1990; Benabdellah et al., 2007; Dafali et al., 2000, 2002; Laarej et al., 2010; Lisac et al., 1992; Touhami et al., 1999; Tebbji et al., 2007). The choice of these ligands is based specially by the presence of two nitrogen atoms in the cyclic rings. Also the presence of various substitutents which can influence on the active centres of adsorption. The present paper exposes the results obtained in studying the inhibiting effect of a bipyrazolic compound (Fig. 1), synthesised in laboratory (Touzani et al., 2003, 2001; Garbacia et al., 2005; Bouabdallah et al., 2007; ElKodadi et al., 2008) on the copper corrosion in aerated 3% NaCl solution by potentiodynamic and polarisation resistance methods.

2. Experimental methods

The solution of 3% NaCl was prepared with double distilled water. Pure copper (99.9%) was used as the working electrode. A platinum counter electrode and a saturated calomel electrode (SCE) as reference electrode were used. Previous to all polarisation runs, the rotating disc electrode (RDE) at 100–3000 rpm was immersed in the test solution for 60 min. The potential scan rate was 30 mV min^{-1}. Effect of the concentration inhibitor was undertaken at 1000 rpm. Polarisation resistance measurements were performed by scanning through a potential range (± 10 mV) which is very close to the corrosion potential. Electrochemical experiments were performed with an Amel potentiostat 449 and the curves were recorded on a Hewlett Packard plotter (more details in (Dafali et al., 2003).

2.1. Computational details

The quantum calculations were performed using the GAUSSIAN 03 program (Frisch, 2003). The geometry of the studied compound was evaluated using the DFT level of the three-parameter compound functional of Becke (B3LYP) (Hinchliffe, 1994). The 6-31G* basis set was used for all atoms. The geom-

etry structure was optimised under no constraints. We have also examined HOMO and LUMO levels; the energy gap was evaluated as the difference between the HOMO and LUMO due to the MO energies.

3. Results and discussion

Fig. 2 shows the cathodic curves of copper in the naturally aerated chloride solutions at various rotation rates. All cathodic curves present an O$_2$ reduction plateau according to the much known reduction of oxygen as Eq. (1):

$$O_2 + 4e^- + 2H_2O \rightarrow 4OH^- \tag{1}$$

Table 1 gathered the different parameters deduced from Fig. 2 such as E_{corr}, I_{corr} and I_L at different rotation rates of copper electrode. As seen, there is an increase in the cathodic limit current with increasing rotation rate.

It is clear from Fig. 3 that E_{corr} and I_{corr} vary oppositely with the rotation rate of Cu/NaCl interface; the decrease in E_{corr} is accompanied by an increase in I_{corr}. Furthermore, the estimated anodic and cathodic Tafel slopes, b_a and b_c, are around 67 and -125 mV/dec., respectively.

Fig. 4 indicates that there is a linear correlation between I_L and $\Omega^{1/2}$, suggesting that the kinetics of the reduction of oxygen process obeys the Levich relationship throughout the speed range studied (Levich, 1962):

$$I_L = 0.62 \times n \times F \times A \times D^{2/3} \times \Omega^{1/2} \times v^{-1/6} \times C \tag{2}$$

where I_L is the Levich current, n is the number of electrons transferred in the half reaction, F is the Faraday constant, A
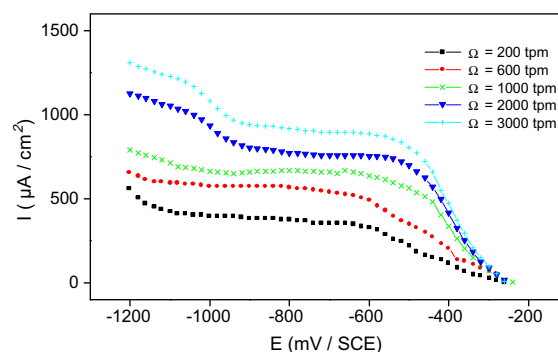
Figure 2   Effect of rotation rate of copper electrode on the cathodic domain.

Table 1   Evolution of E_{corr}, I_{corr} and I_L with the rotation rate of copper electrode.

Ω (rpm)	E_{corr} (mV)	I_{corr} (μA cm^{-2})	I_L (μA cm^{-2})
3000	−270	56	1084
2500	−266	50	990
2000	−264	47	933
1500	−260	45	805
1200	−260	41	763
1000	−257	40	708
800	−251	30	650
600	−245	25	577
400	−247	18	498
200	−242	13	400
100	−248	10	260
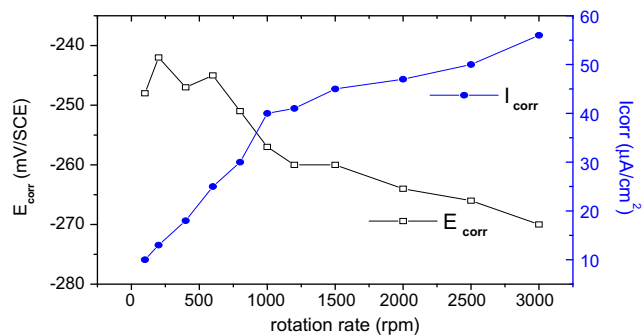
Figure 3 Evolution of E_{corr} and I_{corr} with the rotation rate of Cu/NaCl interface.
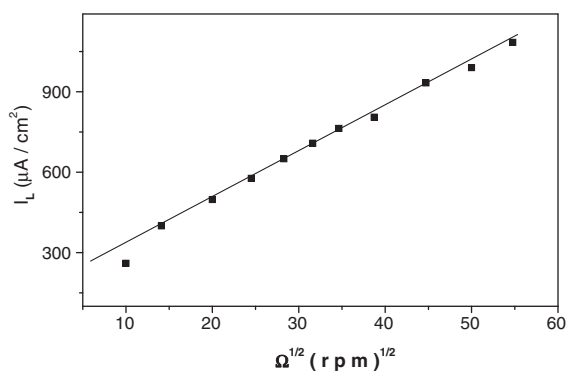
Figure 4 Plot of the logarithm of the limiting current versus the square logarithm of the rotation rate in NaCl 3%: Levich equation.

is the electrode area, D is the diffusion coefficient, Ω is the angular rotation rate of the electrode, v is the kinematic viscosity and C is the concentration of reactant.

We note also that the line does not pass through the origin. This result may introduce the possibility of non-diffusional current superposed to diffusion current:

$$I = I_k + I_L \qquad (3)$$

This proves that the regime at the interface Cu/3% NaCl is laminar hydrodynamic. Here, I_K represents the current in the absence of any mass-transfer effects, that is, the current that would flow under the kinetic limitation if the mass transfer was efficient enough to keep the concentration at the electrode surface equal to the bulk value, regardless of the electrode reaction (Bard and Faulkner, 2001).

Then, the kinetics of the Cu/NaCl interface is a mixed-type process; I_{corr} is obtained by extrapolation of the corrected current I_C to E_{corr}. I_c is calculated using the following relation:

$$\frac{1}{I} = \frac{1}{I_c} + \frac{1}{I_L} \qquad (4)$$

where I is the cathodic current measured (Fig. 2).

3.1. Effect of BiPyA concentration on the corrosion behaviour of Cu/3% NaCl

Fig. 5 illustrates the anodic and cathodic polarisation curves recorded on copper electrodes with and without the bipyrazole
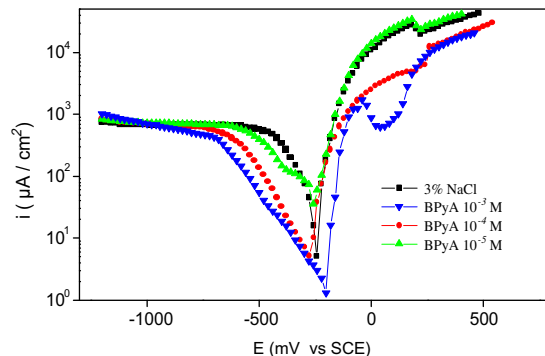
Figure 5 Polarisation curves of copper with and without various concentration of BiPyA in 3% NaCl solution.

tested at different concentrations respectively. The deduced electrochemical parameters are collected in Table 2. The inhibition efficiency ($E\%$) was calculated from polarisation measurements according to the relation:

$$E\% = \frac{I^0_{corr} - I_{corr}}{I^0_{corr}} \times 100 \qquad (5)$$

where I_{corr} and I_{corr} are the corrosion current, density values without and with inhibitor, respectively.

In the presence of BiPyA, at different concentrations, an appreciable change in the nature and behaviour of the cathodic and anodic polarisation curves is observed. The initial increase in current density values was not as rapid as in its absence. The current density values are shifted towards lower values with the increase of the concentration. The effect was maximal at 10^{-3} M in which the inhibition efficiency attains 94.5%. Electrochemical data collected in Table 1 reveal that both E_{corr} and β_c are modified in the presence of inhibitor. E_{corr} shifted to more anodic potentials and β_c changes indicate the modification of the corrosion mechanism.

In the anodic domain, we observe that the existence of BiPyA is characterised by the appearance of weak over voltages of a characteristic bump of the training layer of corrosion products on the surface of copper. This phenomenon may be explained by the possible formation of copper complex as shown in the literature with similar compounds (ElKodadi et al., 2008; Bouabdallah et al., 2007; Vera et al., 2008; Touzani et al., 2011). In these later works, the synthesis of copper II complex with bipyrazolic compounds named tridentate ligands was reported. Abdallah and El-Naggar (2001) have demonstrated the formation of copper II with a pyrazolic compound. In this optic, and according to the literature data of similar bipyrazole derivatives, we may suggest the formation of copper-bipyrazole as shown in Fig. 6.

Linear polarisation resistance values were obtained from current/potential plots. The obtained linear polarisation plots for copper in 3% NaCl in the absence and presence of different concentrations of BiPyA are shown in Fig. 7. The polarisation resistances obtained are also given in Table 2. In this case, the inhibition efficiency is calculated using the charge transfer resistance from Eq. (2):

$$E_{R_p}\% = \frac{R_{p(inh)} - R_p}{R_{p(inh)}} \times 100 \qquad (6)$$

where $R_{p(inh)}$ and R_p are the LPR values in the presence and absence of BiPyA, respectively.

Table 2 Corrosion inhibition parameters of copper in aerated 3% NaCl solution with and without inhibitor at various concentrations at 25 °C.

	E_{corr} (mV/SCE)	b_{cm} (mV/dec)	I_{corr} (μA/cm^2)	E_I (%)	R_p (Ω cm^2)	E_R (%)
Blank	−258	125	40.2	–	620	–
10^{-6} M	−256	170	23.6	41.3	820	24.4
10^{-5} M	−260	176	27.0	32.3	860	27.9
10^{-4} M	−268	165	14.7	63.4	1350	54.1
5.10^{-4} M	−201	175	3.8	90.7	7000	91.1
10^{-3} M	−187	160	2.2	94.5	7750	92.0
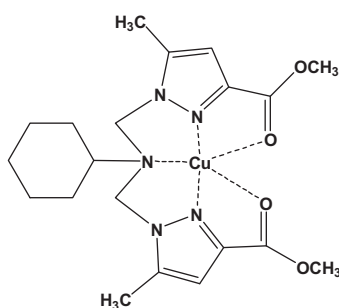
Figure 6   Mechanism suggested of coordination of copper.
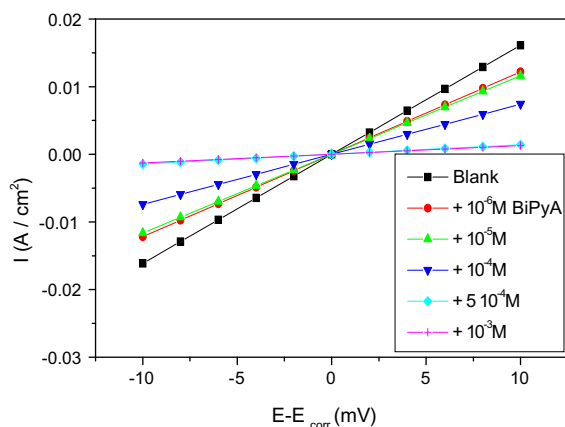
Figure 7   Linear polarisation plots of copper with and without various concentration of BiPyA in 3% NaCl solution around E_{corr}.

LPR parameters of copper/3% NaCl at various concentrations are also given in Table 1. The slope of these curves (R_p) showed an increase in value from 620 Ω cm^2 for the inhibitor free solution to 7750 Ω cm^2 in the presence of 10^{-3} M of the bipyrazole tested. As we may see, the values of R_p, and consequently the corresponding efficiency E_{Rp}, increase with increasing concentrations of the inhibitor indicating that this compound adsorbs on metal surface and inhibits corrosion process.

The inhibition efficiency obtained by the cathodic domain and the other results obtained by polarisation resistance are in good agreement. Adsorption isotherms are very important in determining the mechanism of organic electrochemical reactions. The most frequently used adsorption isotherm is the Langmuir isotherm with the rearranged equation:

$$\frac{C}{\theta} = \frac{1}{K} + C \tag{7}$$

where θ is the surface coverage degree, K is the equilibrium constant of the adsorption process and C is the additive concentration.

The surface coverage values θ were tested graphically for fitting a suitable adsorption isotherm. The plot of C/θ versus C yielded a straight line with a slope 1.03. This was observed clearly proving that the adsorption of the bipyrazole from acid solutions on the copper surface obeys the Langmuir adsorption isotherm (Fig. 8).

The equilibrium constant deduced is 2.54 10^{+6} L/mol. The standard free energy of adsorption ΔG_{ads}°, which can characterise the interaction of adsorption molecules and metal surface, was calculated from the following equation:

$$K = \frac{1}{55.5} \exp\left(-\frac{\Delta G_{ads}^{\circ}}{RT}\right) \tag{12}$$

where R is the universal gas constant and T is the absolute temperature.

The negative value of ΔG_{ads}° means that the adsorption of inhibitor on copper surface is a spontaneous process, and furthermore the negative values of ΔG_{ads}° also show the strong interaction of the inhibitor molecule with the metal surface (Elachouri et al., 1996; Savitri and Mayanna, 1996).

Generally, values of ΔG_{ads}° around −20 kJ mol^{-1} or lower are consistent with the electrostatic interaction between the charged molecules and the charged metal (physisorption). Those more negative than −40 kJ mol^{-1} involve charge sharing or transfer from the inhibitor molecules to the metal surface to form a coordinate type of bond (chemisorption) (Donahue and Nobe, 1965; Khamis et al., 1991). For the investigated inhibitor, the calculated ΔG_{ads}° of −46.61 kJ mol^{-1} indicates that the adsorption mechanism of the bipyrazole on copper in 3% NaCl solution was typical of chemisorption.
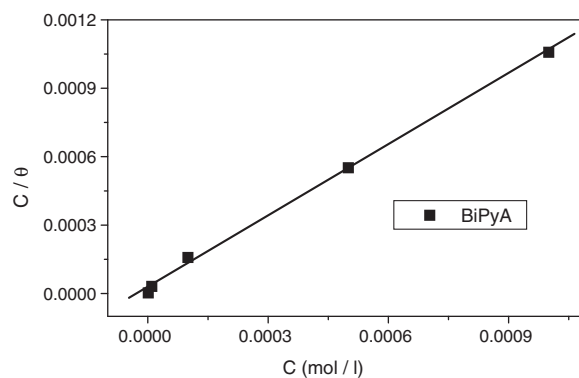
Figure 8   Langmuir isotherm adsorption model of BiPyA on copper surface in 3% Nacl solution.
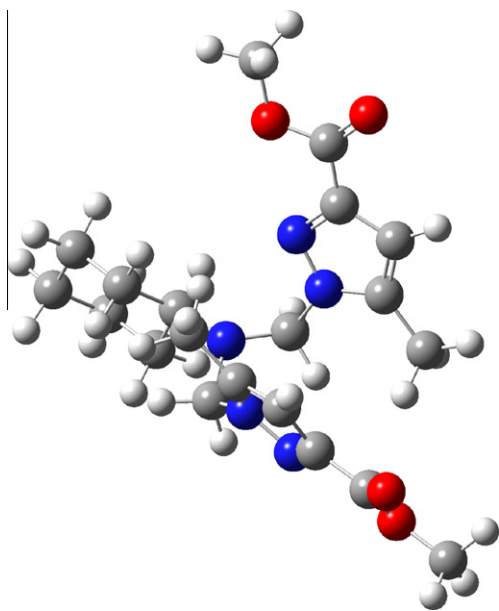
Figure 9 Optimised structure of the studied molecule obtained by B3LYP-6-31 G(d) method.

Table 3 Calculated HOMO (eV), LUMO (eV), ΔE_{gap} (= LUMO − HOMO) (eV), dipole moment (debye) and total energy (u.a.).

E_{HOMO} (eV)	E_{LUMO} (eV)	ΔE (eV)	Dipole moment (Debye)	TE (u.a.)
−6.2100	−0.6753	5.5347	5.2661	−1354.24

4. Quantum chemical calculations

To correlate the experimental data obtained from weight loss, quantum indices of BiPyA are computed using B3LYP/6-31 G(d). The optimised minimum energy structure of BiPyA is shown in Fig. 9.

Among the calculated parameters, we cite energy of the highest occupied molecular orbital (E_{HOMO}), energy of the lowest unoccupied molecular orbital (E_{LUMO}), HOMO–LUMO energy gap (ΔE_{L-H}), dipole moments (debye) and total energy (TE). All energy parameters can also provide an important information about the reactive behaviour of the studied molecule. The resulting data are grouped in the Table 3.

It is known that the value of E_{HOMO} is often associated with the electron donating ability of the inhibitor molecule, higher values of E_{HOMO} is an indication of the greater ease of donating electrons to the unoccupied d orbital of metal. The high values of E_{HOMO} (−6.2100 eV) are likely to indicate a tendency of the molecule to donate electrons to the appropriate acceptor molecules with low energy and empty molecular orbital, whereas the value of E_{LUMO} (−0.6753 eV) indicates its ability of the molecule to accept electrons. Consequently, the value of ΔE_{gap} provides a measure for the stability of the formed complex on the metal surface. The calculated HOMO–LUMO energy gap is 5.534 eV, this small value indicates that BiPyA is a soft molecule and this results in high corrosion inhibition implying soft–soft interaction (Ahamad et al., 2010). Regarding also the total energy as well as the dipole moment, BiPyA may be classified as an efficient inhibitor. Lower the value of ΔE, higher the stability for the formed complex.

In Fig. 10, there is representation of the HOMO and LUMO orbitals calculated form the optimised structure of Bi-PyA by B3LYP-6-31 G(d) method. When the HOMO orbital for BiPyA is analyzed, it is found that the highest occupied molecule orbital (HOMO) is located in the pyrazole ring, and in the functional groups attached to this ring. This would indicate that the preferred active sites for an electronic attack and the favourite sites for interaction with the metal surface are located within the region around the nitrogens belonging to the pyrazole ring.

5. Conclusion

The choice of BiPyA for a detail study allowed reaching the following conclusions:

* The corrosion behaviour of Cu/3% NaCl is laminar hydrodynamic.
* The diffusion of dissolved oxygen to the Cu surface obeys the Levich law.
* The addition of the BiPyA to a corrosive medium decreases the cathodic and anodic currents.
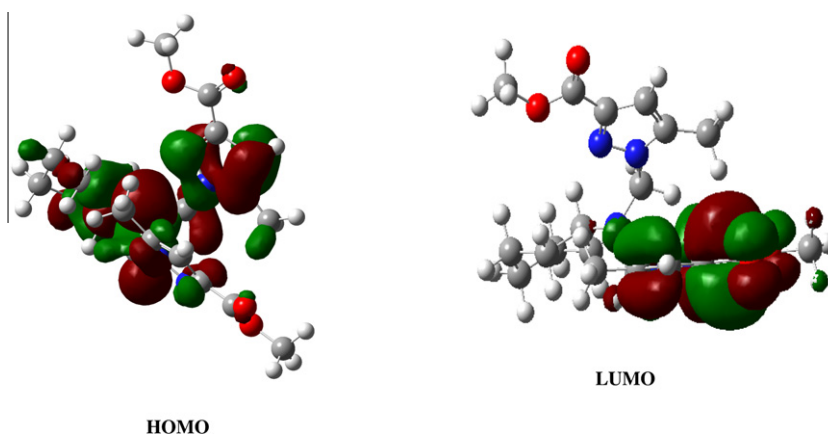
HOMO

LUMO

Figure 10 HOMO and LUMO orbitals of BiPyA.

* The increase of the BiPyA concentration leads to a huge decrease of the corrosion current density and consequently the inhibition efficiency increases to reach about 95% at 10^{-3} M.

* The adsorption of BiPyA on the copper surface obeys the Langmuir adsorption isotherm model.

* The inhibition efficiency of the inhibitor BiPyA is closely related to the DFT quantum chemical parameters, (E_{HOMO}), energy of lowest unoccupied molecular orbital (E_{LUMO}), HOMO–LUMO energy gap (ΔE_{L-H}), dipole moments and total energy (TE).

* The study of the HOMO and LUMO orbitals indicates that the preferred active sites for an electronic attack and the favourite sites for interaction with the metal surface are located within the region around the nitrogenes belonging to the pyrazole ring.

References

Abdallah, M., El-Naggar, M.M., 2001. Cu^{+2} cation + 3,5-dimethyl pyrazole mixture as a corrosion inhibitor for carbon steel in sulfuric acid solution. Mater. Chem. Phys. 71, 291.

Ahamad, I., Prasad, R., Quraishi, M.A., 2010. Experimental and theoretical investigations of adsorption of fexofenadine at mild steel/hydrochloric acid interface as corrosion inhibitor. J. Solid State Electrochem. 14, 2095.

Aouniti, A., Hammouti, B., Brighli, M., Kertit, S., Berhili, F., El Kadiri, S., Ramdani, A., 1996. Inhibition of the acid corrosion of iron with new pyrazole derivatives. J. Chim. Phys. 93, 1262.

Badawy, W.A., Hefny, N.M., El Egamy, S.S., 1990. Effect of some organic amines as corrosion inhibitors for lead in 0.3 M HCl solution. Corros. Sci. 36, 978.

Bard, A.J., Faulkner, L.R. 2001. Electrochemical methods: fundamentals and applications, 2nd ed., ISBN 0-471-04372-9, p. 341.

Benabdellah, M., Touzani, R., Aouniti, A., Dafali, A., El Kadiri, S., Hammouti, B., Benkaddour, M., 2007. Inhibitive action of some bipyrazolic compounds on the corrosion of steel in 1 M HCl. Part I: electrochemical study. Mater. Chem. Phys. 105, 373.

Bouabdallah, I., Touzani, R., Zidane, I., Ramdani, A., 2007. Synthesis of new tripodal ligand: N,N-bis[(1,5-dimethylpyrazol-3-yl)methyl]benzylamine. Catecholase activity of two series of tripodal ligands with some copper (II) salts. Catal. Commun. 8, 707.

Dafali, A., Hammouti, B., Aouniti, A., Mokhlisse, R., Kertit, S., Elkacemi, K., 2000. 2-Mercapto-1-methylimidazole as corrosion inhibitor of copper in aerated 3% NaCl solution. Ann. Chim. Sci. Matér. 25, 437.

Dafali, A., Hammouti, B., Touzani, R., Kertit, S., Ramdani, A., El Kacemi, K., 2002. Corrosion inhibition of copper in 3 per cent NaCl solution by new bipyrazolic derivatives. Anti Corr. Meth. Mater. 49, 96.

Dafali, A., Hammouti, B., Mokhlisse, R., Kertit, S., 2003. Substituted uracils as corrosion inhibitors for copper in 3% NaCl solution. Corros. Sci. 45, 1619.

Donahue, F.M., Nobe, K., 1965. Theory of organic corrosion inhibitors. J. Electrochem. Soc. 112, 886.

Elachouri, M., Hajji, M.S., Salem, M., Kertit, S., Aride, J., Coudert, R., Essassi, E., 1996. Some nonionic surfactants as inhibitors of the corrosion of iron in acid chloride solutions. Corrosion 52, 103.

El Kodadi, M., Malek, F., Touzani, R., Ramdani, A., 2008. Synthesis of new tripodal ligand 5-(bis(3,5-dimethyl-1H-pyrazol-1-ylmethyl)amino)pentan-1-ol, catecholase activities studies of three functional tripodal pyrazolyl N-donor ligands, with different copper (II) salts. Catal. Commun. 9, 966.

Frisch, M.J. et al., 2003. GAUSSIAN 03, Revision B.04, Gaussian, Inc., Pittsburgh PA.

Garbacia, S., Hillairet, C., Touzani, R., Lavastre, O., 2005. New nitrogen-rich tripodal molecules based on bis(pyrazol-1-ylmethyl)amines with substituents modulating steric hindrances and electron density of donor sites. Collec. Czec. Chem. Commun. 70, 34.

Hinchliffe, A., 1994. Modelling Molecular Structures. John Wiley & Sons, New York.

Khamis, E., Bellucci, F., Latanision, R.M., El-Ashry, E.S.H., 1991. Acid corrosion inhibition of nickel by 2-(triphenosphoranylidene) succinic anhydride. Corrosion 47, 677.

Laarej, K., Bouachrine, M., Radi, S., Kertit, S., Hammouti, B., 2010. Quantum chemical studies on the inhibiting effect of bipyrazolees of steel corrosion in HCl. Eur. J. Chem. 7, 419.

Levich, V.G., 1962. Physicochemical Hydrodynamics. Prentice-Hall Inc.

Lisac, E.S., Metikos-Hakovic, M., Lencic, D., Vorkapic-Farac, J., Berkovic, K., 1992. Structural investigation of N-arylpyrroles as iron corrosion inhibitors in hydrochloric acid. Corrosion 48, 1992.

Revie, R.W. 2000. Uhlig's Corrosion Handbook, 2nd ed. ISBN 0-471-15777-5, John Wiley & Sons, Inc.

Savitri, B.V., Mayanna, S., 1996. Tetrabutyl ammonium iodide, cetyl pyridinium bromide and cetyl trimethyl ammonium bromide as corrosion inhibitors for steel. Indian J. Chem. Technol. 3, 256.

Scharnweber, D., 2008. Biodegradation of metals. Ency. Met. Sci. Technol., 555.

Tebbji, K., Bouabdallah, I., Aouniti, A., Hammouti, B., Oudda, H., Benkaddour, M., Ramdani, A., 2007. N-Benzyl-N,N-bis[(3,5-dimethyl-1H-pyrazol-1-yl)methyl]amine as corrosion inhibitor of steel in 1 M HCl. Mater. Lett. 61, 799.

Touhami, F., Hammouti, B., Aouniti, A., Kertit, S., 1999. A new bipyrazolic compound as corrosion inhibitor of armco iron in 1M HCl medium. Ann. Chim. Sci. Mater. 24, 581.

Touzani, R., Ramdani, A., Ben Hadda, T., El Kadiri, S., Maury, O., Le Bozec, H., Dixneuf, P.H., 2001. Efficient synthesis of new nitrogen donor containing tripods under microwave irradiation and without solvent. Synth. Commun. 31, 1315.

Touzani, R., Garbacia, S., Lavastre, O., Yadav, V.K., Carboni, B., 2003. Efficient solution phase combinatorial access to a library of pyrazole- and triazole-containing compounds. J. Comb. Chem. 5, 375.

Touzani, R., Vasapollo, G., Scorrano, S., Del Sole, R., Manera, M.G., Rella, R., El Kadiri, S., 2011. New complexes based on tridentate bipyrazole ligand for optical gas sensing. Mater. Chem. Phys. 126, 375.

Tuck, C.D.S., Powell, C.A., Nuttall, J., 2010. Corrosion of copper and its alloys. Shreir's Corrosion, 1937, Chapter 3.07.

Vera, R., Bastidas, F., Villarroel, M., Oliva, A., Molinari, A., Ramírez, D., Del Río, R., 2008. Corrosion inhibition of copper in chloride media by 1,5-bis(4-dithiocarboxylate-1-dodecyl-5-hydroxy-3-methylpyrazolyl)pentane. Corros. Sci. 50, 729.